

Quasi-zero-dimensional states in ballistic quantum wires

Toshihiro Itoh, Nobuyuki Sano, and Akira Yoshii

NTT LSI Laboratories, 3-1 Morinosato-wakamiya, Atsugi-shi, Kanagawa-ken 243-01, Japan

(Received 14 December 1992)

We study transport properties of ballistic quantum wires in which transverse modes of electrons are strongly mixed. It is shown that there are zero-dimensional quasibound states in these structures. The conductance reflects the existence of these states in two ways: one is a transmission peak and the other a dip. These two distinctive features appear due to the background conductance.

Recent progress in microfabrication techniques, such as planar process or epitaxial growth, has made it possible to observe quantum effects in semiconductors with effective low-dimensional structures.¹ When the electrons are confined in every dimension, discrete zero-dimensional (0D) states are formed and the strongest quantum effects are expected. Recently, transport properties of such systems have been extensively investigated in both lateral²⁻⁵ and vertical^{6,7} structures. In both structures, the analyses are mainly based on the picture of the resonance tunneling in which the conductance reaches a maximum when the Fermi energy coincides with discrete levels of the quantum box. However, when a strong magnetic field^{4,5} inducing adiabatic transport is absent and the mixing of modes cannot be neglected, the transport properties are severely affected by mode mixing, so the simple one-dimensional picture mentioned above is insufficient.⁸

Although vertical structures have the advantage of thin barriers that can be fabricated by an epitaxial technique, the cross section cannot be well formed and it is difficult to see the effect of the mode couplings in this structure. Moreover, current-voltage characteristics are usually analyzed in the nonlinear region, and electron-electron interaction directly affects the transport.^{4,9} On the other hand, in the lateral structure, it is hard to make well-formed thin potential barriers using the gate voltage in order to make the 0D states well defined and to allow appreciable electron transmission.¹ Transverse momentum, however, is well defined in the lateral structure and the linear-response regime can be examined by changing the system size or Fermi energy using the gate voltage. Therefore, the lateral structure is more useful in investigating the effects of mode coupling if the potential barrier is not introduced into the wire.

Some authors examined lateral structures experimentally without introducing a magnetic field or a potential barrier in the wire.^{3,10,11} Hirayama and Saku investigated double-ballistic point-contact geometry. In their analyses, they suggested that transmission through the 0D states occurred.³ Wu *et al.* observed resonance effects in the conductance of double-bend structures.¹⁰ These wires have been analyzed numerically and the conductance of these wires has been reported.^{12,13} However, there is still no clear explanation because such analyses are usually based on the transport coefficient or conductance. It is rather difficult to obtain a physical picture of the trans-

port process by only examining this quantity. Also, it is not clear whether 0D states are well defined in such unbounded structures.

Recently, we introduced the local density of states per unit length and its expansion, in terms of the transverse momentum, to analyze a wire with a stub.^{14,15} The direct comparison of these quantities with the transport coefficient allows us to see if the increase in conductance merely reflects the increase in the density of states. Moreover, the expansion of the local density of states, in terms of the transverse momentum, gives an insight into the nature of the wave function that constructs the local density of states. This approach is extended to the analyses of wires with a long stub or a double bend, where the transverse modes strongly mix and cannot be defined continuously throughout the wire. We will show that well-defined quasi-zero-dimensional states can be formed in such ballistic quantum wires and that the transport properties of these wires reflect the existence of these states either as a reflection or a transmission.

Our calculational method is the tight-binding Green-function method introduced by Sols *et al.*,¹² which is an extension of the conventional recursive Green-function method.¹⁶ The detailed procedure for the calculations is given elsewhere.^{12,14} We define the local density of states per unit length $D_w(r_x, E)$, and the local density of states per unit length for modes at $r_x, \rho_m(r_x, m_y, E)$, as

$$D_w(r_x, E) = \sum_{r_y} \rho(\mathbf{r}, E) = \sum_{m_y} \rho_m(r_x, m_y, E), \quad (1)$$

$$\rho_m(r_x, m_y, E) = \sum_n \delta(E - E_n) \varphi_n(r_x, m_y) \varphi_n^*(r_x, m_y), \quad (2)$$

$$\varphi_n(r_x, m_y) = \sum_{r_y} f_{m_y}(r_y) \phi_n(r_x, r_y), \quad (3)$$

where $\phi_n(\mathbf{r})$ and E_n are the complete sets of orthonormal eigenfunctions and eigenvalues for the Hamiltonian H , respectively. The eigenfunction with respect to the transverse mode m_y is $f_{m_y}(r_y)$, and $\rho(\mathbf{r}, E)$ is the local density of states per unit area. The system considered is the modulation-doped GaAs-Al_xGa_{1-x}As heterostructure, and the effective mass m^* of GaAs is thus taken to be $0.067m_0$, where m_0 is the rest mass of an electron. The energy is measured from the bottom of the two-dimensional tight-binding band. The spin degeneracy is taken into account in both the conductance and the den-

sity of states.

First, we investigated the stub structure depicted in the inset of Fig. 1(a). The conductance g is shown in Fig. 1(a) as a function of Fermi energy E . The solid line represents the result of the lattice spacing of $a = 1.25$ nm and the dashed line represents that of $a = 0.625$ nm. It is clear that the lattice spacing of 1.25 nm has sufficient accuracy for our purpose. We therefore use a lattice spacing of $a = 1.25$ nm throughout our calculations. The conductance profile shows an irregularly oscillating structure, implying strong mixing of transverse modes. In addition, five narrow dips located at $E = 3.7, 6.8, 9.0, 20.2,$ and 21.9 meV were observed. To clarify the origin of these dips, the local density of states per unit length for modes $D_w(r_x, E)$ at position C [see the inset to Fig. 1(a)] is plotted in Fig. 1(b). Well-defined peaks, which are regarded as quasibound states, are clearly seen. Comparing Figs. 1(a) and 1(b), the first, second, and fifth dips, in the conductance profile, have corresponding peaks in the local density of states. Although such correspondence is also observed in the wire with a short stub,¹⁴ there is a clear difference. In Fig. 1(b), the quasi-one-dimensional subband spectrum, which has dependency of $(E - E_n)^{-1/2}$

and corresponds to extended states, is not observed. E_n is the propagation threshold of the n th subband.

To investigate these quasibound states in more detail, $D_w(r_x, E)$ was expanded in terms of transverse momentum m_y . The result at position C , denoted as $\rho_m(r_x, m_y, E)$, is shown in Fig. 1(c). While the peak at 3.7 meV breaks into two modes and the peak at 21.9 meV into three modes, the other three peaks remain as single modes. Subsequently, let us compare the energy that creates the peak for each mode with the discrete eigenenergy of the virtual quantum box, which is represented by the rectangle bounded by dot-dashed lines in the inset of Fig. 1(a). The eigenenergy is marked by lines on the top of Fig. 1(c) and is represented by $E_{m_x m_y} = \hbar^2 / 2m^* \{ (m_x / 2W_x)^2 + (m_y / 2W_y)^2 \}$, where W_x and W_y are the length of the box in the x and y directions, respectively. From the figure, a correspondence is observed, except for the peaks corresponding to $m_x = 2$. This is because $\rho_m(r_x, m_y, E)$ is calculated at C where the wave function with even mode has a node. This will be shown in detail later.

Since the leads are attached to the virtual quantum box, the states of the quantum box acquire finite probabilities of decaying outside the box. As a result, these states acquire finite width and become quasibound states. The lifetimes of these quasibound states are governed by the couplings at the interface and can be estimated from the width of these peaks by using the uncertainty principle. The lifetimes of these states are on the order of 1 ps. The positions of the peaks also shift from the discrete levels as the quasibound states at the peaks extend over the larger region. Only the lowest state remains as a real bound state. This is confirmed by evaluating the real diagonal part of the Green function.^{12,14} The energy of this real bound state is shown by an arrow in Fig. 1(b) and agrees with the results in Sols *et al.*¹² The real bound state and the lowest quasibound state are considered to result from the combination of E_{11} and E_{12} .

Since the transverse modes change at the interface, the local density of states per mode is not necessarily continuous. The sum over the modes, $D_w(r_x, E)$, however, is continuous even at the interface. To clearly show the difference in the local electronic structure between the inside and outside regions of the stub, $D_w(r_x, E)$ was calculated for both regions. The results are shown in Fig. 2, where Fig. 2(a) shows the stub region and 2(b) the lead region. As expected, a quasi-one-dimensional subband spectrum, which is the sum of $(E - E_n)^{-1/2}$, is seen in Fig. 2(b). The oscillating structure is attributed to partial reflection of the electron waves at the interface. Figure 2(a) shows a quite different profile from Fig. 2(b); the amplitude increased strikingly at the quasibound states, which means that these states are likely to be confined within the box. The mode index m_x of these quasibound states can be determined by the number of peaks along the r_x direction. Note that the amplitude of the two quasibound states at $E = 9.0$ and 20.2 meV become nearly zero at $r_x = 25$ nm and they are not visible in Figs. 1(b) and 1(c). These quasibound states have the mode index of $m_x = 2$ and correspond to the third and the fourth dips in

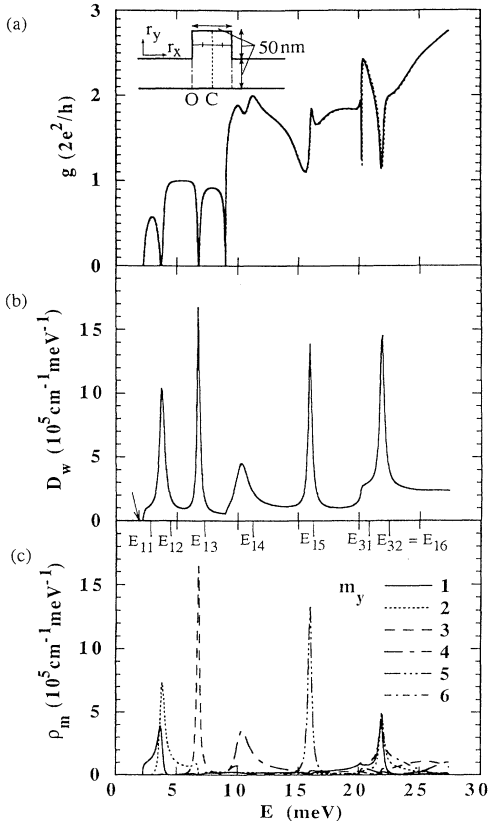


FIG. 1. (a) Conductance g : lattice spacing of 1.25 nm (solid line) and 0.625 nm (dashed line). Inset: The structure with a stub. The dashed line represents position C . O is the origin of r_x . The dot-dashed lines indicate the region of the virtual quantum box. (b) $D_w(r_x, E)$ at C in the inset of Fig. 1(a). (c) $\rho_m(r_x, m_y, E)$ at C for $m_y = 1$ to 6, for a stub structure.

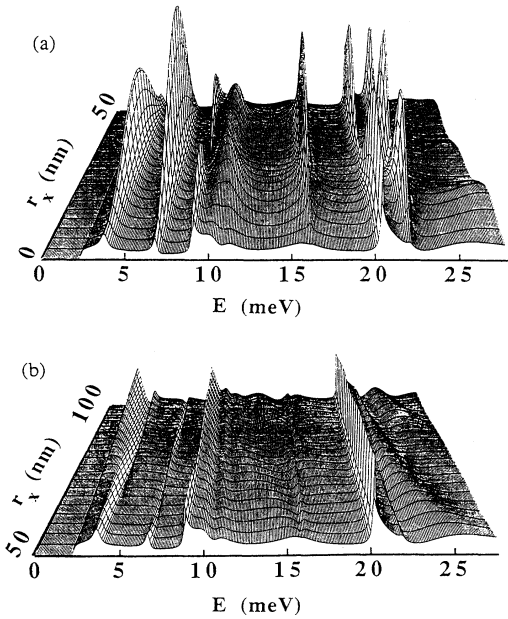


FIG. 2. Local density of states per unit length $D_w(r_x, E)$ vs energy E and position r_x (a) in the stub and (b) outside the stub. r_x is taken from the origin O in the inset of Fig. 1(a).

Fig. 1(a). Therefore, all dips in the conductance have the corresponding quasibound states at the same energy.

These dip characteristics have also been observed when the small stub or an attractive potential was introduced into the wire.^{17,14} In such systems, the dips are explained by the quasibound states splitting off from higher-lying confinement subbands. In a system with a long stub, however, width discontinuity is so large that there is no one-to-one correspondence of the transverse modes between the stub and the wire regions, and strong reflection of the electron wave occurs at the interface. Consequently, to explain the nature of these quasibound states, a picture based on the levels of the quantum box employed here is much more appropriate than the picture in terms of the quasibound states splitting off from the propagating modes. Therefore, the device proposed by Sols *et al.*¹² can be regarded as a zero-dimensional device controlling the discrete levels of a quantum box, rather than a one-dimensional device controlling the phase of the modes.

Next, the double-bend structure, which is shown in the inset of Fig. 3(a), was investigated. In this case, quasibound states contribute differently to the transport properties of the wire than in the case of the long stub. The conductance g is plotted in Fig. 3(a). Although the curve shows an oscillatory structure similar to Fig. 1(a), there is a clear difference. In the curve shown in Fig. 1(a), the narrow dips are dominant, while the peaks dominate the curve in Fig. 3(a). The nine peaks are observed at 2.8, 4.0, 5.5, 7.1, 8.5, 9.3, 11.4, 13.6, and 18.8 meV. To investigate these characteristics in more detail, the local density of states $D_w(r_x, E)$ was calculated and is shown in Fig. 3(b). The peaks in Fig. 3(a), except that of 9.3 meV, have corresponding peaks in Fig. 3(b). This characteristic con-

trasts to that of the stub structure where peaks are found at the energy of the dips in the conductance. In the double-bend structure, quasibound states contribute directly to the current, and the transmission occurs through these states. In the single-mode regime ($E < 9$ meV) in particular, the maximum conductance reaches unity for five peaks. This feature of the conductance is similar to that of resonance tunneling in one dimension. Figure 3(c) shows the expansion of $D_w(r_x, E)$ in terms of the transverse modes of the central region. Comparing Figs. 3(b) and 3(c), most of the peaks in Fig. 3(b) result from single modes, whereas the first peak in Fig. 3(b) consists of three modes. As seen previously in the system with a stub, clear correspondence is observed between the quasibound states and the discrete levels of the virtual quantum box, indicated by dot-dashed lines in the inset of Fig. 3(a). In investigating the real part of the Green function, two real bound states were found for this system.¹⁸ These states and the lowest quasibound state are considered to originate from the combination of the three lowest levels of the quantum box. In Fig. 3(a), two dips are also observed at $E = 16.1$ and 25.9 meV. They have corresponding quasibound states at the same energy [Fig. 3(b)], and their origin is considered to be the same as the

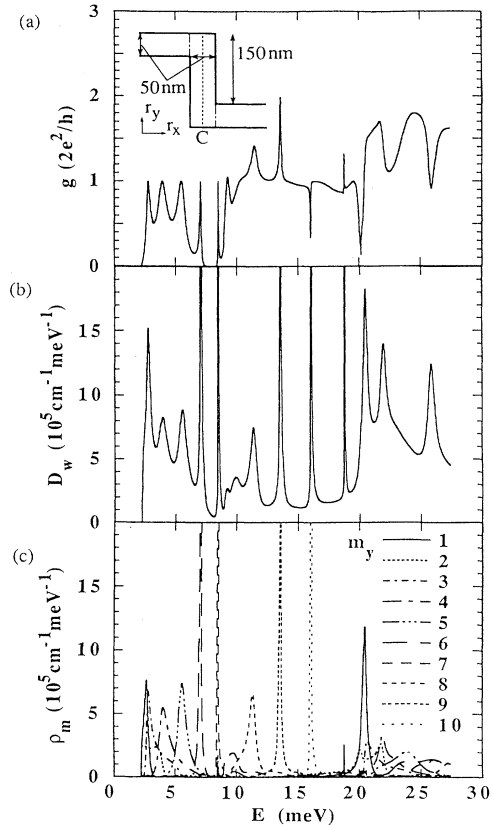


FIG. 3. (a) Conductance g : Inset: the structure with a double bend. The dashed line represents position C . The dot-dashed lines indicate the region of the virtual quantum box. (b) $D_w(r_x, E)$ at C in the inset of Fig. 3(a). (c) $\rho_m(r_x, m_y, E)$ at C for $m_y = 1-10$, for a double-bend structure.

dips in the system with a stub.

In the two structures presented here, it is seen that “zero-dimensional” quasibound states appear in the conductance profile in two ways: one as transmission and the other as reflection. This feature is analogous to that explained by Nakazato and Blaikie¹⁷ in the case of weak mode mixing. When the lower mode is opened, the back-scattering lower mode contributes as a dip, and the higher mode contributes as a peak when the lower mode is closed. In this case, however, these quasibound states couple strongly with both the propagating lower mode and the evanescent higher mode. Therefore, it is not possible to classify the quasibound states by the subband indices in the leads. In the real systems, because of the wider width of these quasibound states, these states are expected to be observed more easily than in the case of weak mode mixing.

Although the analysis presented so far has been restricted to the coherent process and we have not taken

electron-electron interaction into account, we can consider that one-electron analysis is applicable to the interacting electron systems, as far as the linear response regime is concerned.⁴ Therefore, it is considered that the structures presented in this paper will provide a way to observe quasi-zero-dimensional states in ballistic quantum wires. In fact, the resonance structure observed by Wu *et al.*¹⁰ would imply the occurrence of the resonance transmission through these states.

To conclude, we analyzed ballistic quantum wires with a stub or a double bend. We showed that quasibound states arise in geometrically unbounded systems and that they correspond to discrete levels of the virtual quantum box in a wire. These “quasi-zero-dimensional” quasibound states appear differently in the transport properties in these two structures.

The authors would like to thank M. Yamamoto for helpful discussions and K. Hirata for his encouragement.

¹C. W. J. Beenakker and H. van Houten, in *Solid State Physics*, edited by H. Ehrenreich and D. Turnbull (Academic, New York, 1991), Vol. 44, p. 1.

²C. G. Smith *et al.*, *J. Phys. C* **21**, L893 (1988).

³Y. Hirayama and T. Saku, *Phys. Rev. B* **41**, 2927 (1990).

⁴A. T. Johnson *et al.*, *Phys. Rev. Lett.* **69**, 1592 (1992).

⁵B. J. van Wees *et al.*, *Phys. Rev. Lett.* **62**, 2523 (1989).

⁶M. A. Reed *et al.*, *Phys. Rev. Lett.* **60**, 535 (1988).

⁷S. Tarucha, Y. Tokura, and Y. Hirayama, *Phys. Rev. B* **44**, 13 815 (1991).

⁸G. W. Bryant, *Phys. Rev.* **44**, 12 837 (1991).

⁹A. Groshev, *Phys. Rev. B* **42**, 5895 (1990).

¹⁰J. C. Wu *et al.*, *Appl. Phys. Lett.* **59**, 102 (1991).

¹¹K. Aihara, M. Yamamoto, and T. Mizutani, *Jpn. J. Appl. Phys.* **31**, L916 (1992).

¹²F. Sols *et al.*, *Appl. Phys. Lett.* **54**, 350 (1989); *J. Appl. Phys.* **66**, 3892 (1989).

¹³A. Weisshaar *et al.*, *Appl. Phys. Lett.* **55**, 2114 (1989).

¹⁴T. Itoh, N. Sano, and A. Yoshii, *Phys. Rev. B* **45**, 14 131 (1992).

¹⁵T. Itoh, N. Sano, and A. Yoshii (unpublished).

¹⁶D. J. Thouless and S. Kirkpatrick, *J. Phys. C* **14**, 235 (1981); P. A. Lee and D. S. Fisher, *Phys. Rev. Lett.* **47**, 882 (1981).

¹⁷C. S. Chu and R. S. Sorbello, *Phys. Rev. B* **40**, 5941 (1989); P. F. Bagwell, *ibid.* **41**, 10 354 (1990); E. Tekman and S. Ciraci, *ibid.* **43**, 7145 (1991); H. Kasai, K. Mitsutake, and A. Okiji, *J. Phys. Soc. Jpn.* **60**, 1679 (1991); K. Nakazato and R. J. Blaikie, *J. Phys. Condens. Matter* **3**, 5729 (1991).

¹⁸H. Wu, D. W. L. Sprung, and J. Martorell, *Phys. Rev. B* **45**, 11 960 (1992).